Ab initio methods for finite-temperature two-dimensional Bose gases

S. P. Cockburn and N. P. Proukakis

Joint Quantum Centre (JQC) Durham-Newcastle, School of Mathematics and Statistics, Newcastle University, Newcastle upon Tyne NE1 7RU, United Kingdom

(Received 29 June 2012; revised manuscript received 27 August 2012; published 10 September 2012)

The stochastic Gross-Pitaevskii equation and modified Popov theory are shown to provide an excellent *ab initio* description of finite-temperature, weakly interacting, two-dimensional Bose gas experiments. In particular, we demonstrate that the stochastic Gross-Pitaevskii equation generates excellent agreement with the recent experiment by C.-L. Hung *et al.* [Nature **470**, 236 (2011)], thereby confirming that the observed universality and scale invariance arise naturally within this formalism. This is achieved in an *ab initio* manner, in which a systematic approach for obtaining a suitable value for the momentum cutoff of interacting classical field theories is proposed by means of the modified Popov theory.

DOI: 10.1103/PhysRevA.86.033610 PACS number(s): 67.85.Bc, 03.75.Hh

I. INTRODUCTION

Ultracold atomic gases represent versatile tools with which to investigate many-body quantum physics [1]. A key tunable property of these systems is their effective dimensionality; increasing the trapping potential, used in experiments to confine and cool atoms, in one or two directions produces gases that are effectively two-dimensional (2D) or one-dimensional (1D), respectively. Low-dimensional geometries in turn lead to richer physics due to the enhanced importance of fluctuations which restrict the onset of long-range order [2,3].

A number of experiments have been performed recently in order to examine the thermodynamic properties of weakly interacting 2D Bose gases [4–13]. Due to the high precision now routinely attained in such experiments, a particularly powerful feature is their usefulness in accurately testing microscopic theories. In this respect, the 2D Bose gas is interesting, as fluctuations are typically important over a broad critical region [14,15], meaning that the standard mean-field approach to weakly interacting Bose gases is not well suited; this broadness was, however, exploited by Hung *et al.* [13] to obtain a clear experimental observation of critical phenomena in ultracold atoms near the Berezinskii-Kosterlitz-Thouless (BKT) phase transition [16,17].

At equilibrium, Monte Carlo (MC) calculations have been successfully applied to the uniform 2D Bose gas [14,18,19], notably yielding a microscopic prediction for the BKT transition point [19]. The harmonically trapped case has been studied using quantum MC [20], various mean-field theories [21–25], and classical field calculations [26–28]. Classical field methods have the advantage of providing a time-dependent description of the gas, which makes them additionally applicable to systems away from equilibrium; nonetheless, a simple yet accurate mean-field theory is also highly desirable to avoid the need for more complicated methods in calculating equilibrium properties. In this work we perform a quantitative comparison between two such complementary methods: (i) the modified Popov (MP) theory of Stoof and co-workers [29,30], which is straightforward to solve and provides quick access to equilibrium properties in all dimensions; and (ii) the stochastic Gross-Pitaevskii equation (SGPE) [31–33] (see also [34]), which has already successfully described several 1D Bose gas experiments [35,36] and is also applicable in dynamical situations [32,37]. The experimental *in situ* measurements by Hung *et al.* [13] offer an ideal test bed for the theories we wish to consider, free of the complications associated with modeling expansion imaging, thus a primary motivation for this work is to demonstrate the applicability of the SGPE in capturing the universality and scale invariance of 2D experiments.

A further related aim is to offer a way of systematically circumventing a standard limitation of classical field calculations, linked to the fact that the Bose gas represented in this way must obey classical statistics. In practical terms, this issue manifests as a sensitivity to the momentum or energy cutoff used in solving such models [38,39], which, as a free parameter, can undermine their use for *ab initio* studies. While calculations based upon classical lattice models have been linked back to their quantum counterparts in the context of MC studies [19,40], the choice of such a cutoff is less clear for methods based upon *dynamical* equilibration of classical fields: approaches to date include selecting a cutoff based on the assumption that the classical field temperature should match that of an *ideal* Bose gas with the same condensate fraction [41], specifying a minimum acceptable mode occupation, typically within an energy cutoff somewhere in the range $g_{2D}n < E_{\rm cut} \lesssim k_BT$ [39], and a high temperature semiclassical field method valid for $k_BT > \mu$ [42].

Motivated by the desire for a formulaic approach to cutoff choice that is valid also at temperatures $k_BT \lesssim \mu$, and that includes the effect of interactions, in this work we discuss and test a systematic strategy for cutoff choice, based upon comparing the classical and quantum limits of MP theory. By studying the sensitivity to cutoff variations around our proposed value (Appendix A), we demonstrate that our technique generates an excellent *ab initio* systematic way of numerically choosing an "optimum" cutoff in the classical theory—to the extent that any cutoff choice in a classical field theory can capture the properties of the inherently quantum physical system—which indeed accurately reproduces important features observed experimentally [13]; moreover, results for a particular cutoff are shown (Appendix B) to be obtained independently from the actual numerical discretization used in the simulations.

II. METHODOLOGY

The 2D SGPE describes the Bose gas via a noisy field $\psi(\mathbf{x},t)$, which satisfies the equation of motion

$$i\hbar\frac{\partial\psi(\mathbf{x},t)}{\partial t} = [1-i\gamma(\mathbf{x},t)]\Big[-\frac{\hbar^2}{2m}\nabla^2_{x,y} + V(\mathbf{x}) - \mu + g_{2D}(|\psi(\mathbf{x},t)|^2 + 2n_{\rm above}(\mathbf{x}))\Big]\psi(\mathbf{x},t) + \eta(\mathbf{x},t), \tag{1}$$

where $V(\mathbf{x}) = m\omega^2(x^2+y^2)/2 = m\omega^2 r^2/2$ is the trapping potential in the more weakly confined x-y plane, $g_{2D} = \sqrt{8\pi}(a/l_z)\hbar^2/m = g\hbar^2/m$ is the 2D interaction strength (with a the s-wave scattering length), and η is a complex Gaussian noise term, with correlations given by the relation $\langle\eta^*(\mathbf{x},t)\eta(\mathbf{x}',t')\rangle = 2\hbar\gamma(\mathbf{x},t)k_BT\delta(\mathbf{x}-\mathbf{x}')\delta(t-t')$. In Eq. (1) $n_{\rm above}$ denotes the density of atoms with momenta greater than the momentum cutoff due to the numerical grid used to solve the SGPE [43].

Classical field methods arise following the observation that the Bose field operator may be accurately replaced in the Heisenberg equation of motion by a complex valued field, under the condition that system modes represented in this way are highly occupied. Although this is an excellent approximation in many circumstances, the system is then found to obey Rayleigh-Jeans statistics at equilibrium. In arriving at Eq. (1), a similar notion is embodied in moving to a classical fluctuation-dissipation theorem (see Eqs. (38)–(40) in Ref. [33]).

The numerical solution to Eq. (1) introduces an ultraviolet momentum cutoff implemented here by the discretization scheme chosen; this implies that the equilibrium thermal state that is achieved for a given set of physical parameters can differ quite dramatically through variation of the grid spacing alone. There is then clearly some ambiguity in making a cutoff choice, and so to address this point for 2D Bose gases, we choose to make use of the MP theory.

The MP theory [29,30] was formulated specifically to describe low-dimensional Bose gases, taking into account the effects of phase fluctuations to all orders [29], and has been found to agree well with the SGPE in previous studies [30,44,45]. In Ref. [23], MP results were compared to both Hartree-Fock (HF) and MC results for a 2D Bose gas. The MP predictions for the critical chemical potential and density for the BKT transition were in excellent agreement with those obtained from MC simulations [19]. In fact, the MP theory was found only to break down in the region where its equation of state reduces to that of HF, which occurs close to the BKT transition due to the mean-field nature of this approach. A renormalization-group analysis was subsequently shown to avoid this discontinuity and to match smoothly to the MP equation of state for chemical potentials, $\mu > 0.18k_BT$ [23].

The central object within the MP approach is the quasicondensate [46], which, in the Thomas-Fermi approximation, obeys $g_{2D}(n_{\rm qc}+2n_{\rm t}) = \mu_{\rm eff}$, where the effective chemical potential may be written as $\mu_{\rm eff} = \mu - V(\mathbf{x})$. The thermal density is calculated from [29,30]

$$n_t = n_{\rm qc} + \frac{1}{V}\sum_{\mathbf{k}=0}^{\mathbf{k}_{\rm max}}\left\{\frac{\epsilon_{\mathbf{k}}}{2\hbar\omega_{\mathbf{k}}}[2N_{\mathbf{k}}+1] - \frac{1}{2} + \frac{g_{2D}n_{\rm qc}}{2\epsilon_{\mathbf{k}}+2\mu}\right\}, \tag{2}$$

with $\hbar\omega_{\mathbf{k}} = \sqrt{\epsilon_{\mathbf{k}}(\epsilon_{\mathbf{k}}+2g_{2D}n_{\rm qc})}$ and $\epsilon_{\mathbf{k}} = \hbar^2\mathbf{k}^2/2m$.

A. Strategy for "optimum" cutoff selection: Classical vs quantum statistics

In the usual formulation of MP, $N_{\mathbf{k}} = N^{\rm BE}_{\mathbf{k}} \equiv 1/(\exp(\beta\hbar\omega_{\mathbf{k}})-1)$, since the particles obey Bose-Einstein statistics, and the upper index in the sum in Eq. (2), $\mathbf{k}_{\rm max}$, may be straightforwardly taken to infinity. However, setting $N_{\mathbf{k}} = N^{\rm RJ}_{\mathbf{k}} \equiv 1/(\beta\hbar\omega_{\mathbf{k}})$ instead leads to a MP result based upon Rayleigh-Jeans statistics, which is therefore analogous to using the classical fluctuation-dissipation result in the SGPE (see, e.g., Eqs. (38)–(40) in Ref. [33]). We use $\rm MP_{RJ}$ and $\rm MP_{BE}$ to denote the Rayleigh-Jeans and Bose-Einstein cases, respectively.

Since the $\rm MP_{RJ}$ approach gives very good agreement with the SGPE for a given cutoff [47], this allows us to extract an "optimum" value for the SGPE grid spacing; this is done here by examining the accuracy of the classical approximation as $\mathbf{k}_{\rm max}$ is varied by directly comparing the $\rm MP_{RJ}$ and $\rm MP_{BE}$ results. To measure this difference, we compare predictions for the normalized second-order correlation function, chosen because of the important role played by density fluctuations in quasicondensation. In the MP theory, this is given by $g^{(2)} = (n^2_{\rm qc}+4n_{\rm qc}n_{\rm t}+2n^2_{\rm t})/(n_{\rm qc}+n_{\rm t})^2$. The procedure we adopt is to first calculate $g^{(2)}(\mathbf{x}=\mathbf{0})$ using the Bose-Einstein distribution in Eq. (2). This value then serves as a target result which we aim to match using the $\rm MP_{RJ}$ with all other parameters held constant. Once a cutoff is selected in this way, it is then used to calculate the numerical grid spacing for use in the SGPE simulations, yielding a combined SGPE-MP approach.

This approach is illustrated in Fig. 1, where symbols indicate the $g^{(2)}(0)$ values obtained from $\rm MP_{BE}$ for two temperatures as the energy cutoff, shown on the horizontal axis as $\beta E_{\rm cut} \equiv \beta\hbar^2|\mathbf{k}_{\rm max}|^2/2m$, is varied. The diagonal dashed lines show the results if we neglect atoms above the cutoff momentum in the $\rm MP_{RJ}$ calculations. The symbols asymptote towards these lines for energy cutoffs $\gtrsim k_BT$, as there are then very few atoms in modes above the cutoff energy. For each temperature, the SGPE-MP energy cutoff may be read off from Fig. 1 as the horizontal coordinate of the point at which the classical $g^{(2)}(0)$ data (squares and circles) intersect the horizontal line indicating the Bose-Einstein result. The lower plots show $g^{(2)}(x)$ and density profiles for the Bose-Einstein calculation [solid (black) lines] and the Rayleigh-Jeans for several cutoffs: $\beta E_{\rm cut} = 0.20$ [dotted (blue) lines], 0.77 [dashed (brown) lines], and 1.50 [dot-dashed (red) lines].

For the *ideal* gas, an expression was derived in Ref. [48] for a cutoff leading to optimum agreement between quantum and classical statistics; in two dimensions, it was found that this occurred at an energy $\beta E_{\rm cut} \approx 1.6$. Using the method outlined above we typically find the best agreement for values around $\beta E_{\rm cut} \approx 0.77$, which varies slowly with temperature in the

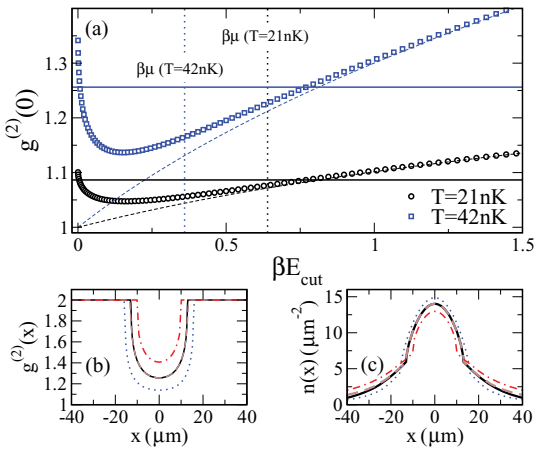

FIG. 1. (Color online) Numerical grid choice. (a) Variation in $g^{(2)}(0)$ with the energy cutoff for $\mathrm{MP_{RJ}}$ at two temperatures. Horizontal lines indicate $\mathrm{MP_{BE}}$ results; the horizontal coordinate of the point at which the $\mathrm{MP_{RJ}}$ data intersect the relevant $\mathrm{MP_{BE}}$ result identifies the energy cutoff that gives the best agreement. Dashed lines indicate the results when above-cutoff atoms are neglected. (b) $g^{(2)}(x)$ and (c) density profiles from $\mathrm{MP_{BE}}$ [solid (black) lines] and $\mathrm{MP_{RJ}}$ for several cutoffs: $\beta E_{\mathrm{cut}} = 0.20$ [dotted (blue) lines], $\beta E_{\mathrm{cut}} \approx 0.77$ [dashed (brown) lines], and $\beta E_{\mathrm{cut}} = 1.50$ [dot-dashed (red) lines].

range considered, yet is clearly much lower than the ideal-gas prediction, indicating the important role of interactions.

III. COMPARISON TO EXPERIMENTAL RESULTS

In order to validate our scheme, we now directly compare the results to *in situ* experimental data of Hung *et al.* [13]. We begin with the $\mathrm{MP_{BE}}$ method and fix the trap parameters and temperature to those quoted in Ref. [13]. We then vary the chemical potential until the required density is reached at the trap center. This provides us with all relevant physical parameters required to solve the SGPE, barring a suitable choice of grid spacing, which is extracted as described; since there are then no free parameters, both the MP theory and the SGPE provide an *ab initio* description of the experiment.

Figure 2 shows the SGPE-MP (i.e., the SGPE with a cutoff obtained by comparing $\mathrm{MP_{RJ}}$ and $\mathrm{MP_{BE}}$ results as described) and MP results together with the experimental density profiles in Ref. [13]. (Note that, as all experimental results were reported as a function of the radial distance, for clarity we also henceforth label our axis r.) Corresponding data for density fluctuations, obtained from the normalized second-order correlation function $g^{(2)}(r)$ via $\langle \delta n^2(r) \rangle = (g^{(2)}(r) - 1)\langle n(r) \rangle^2$ upon averaging over 1000 independent realizations, are shown in the bottom row in Fig. 2. By comparison also to HF [49], the trend we observe is that, despite matching the experimental density profiles well, the HF results consistently predict density fluctuations that are too large, relative to those observed experimentally. This may be understood since energy reducing correlations which lead to the onset of quasicondensation are not incorporated in this theory, in accordance with the findings for highly elongated gases presented in Ref. [50]. In contrast, the SGPE and MP data agree very well with the experimental findings, thereby confirming the utility of each in describing the physics of 2D Bose gases at finite temperatures.

Moreover, these findings highlight that choosing a grid spacing based upon a higher order field correlation such as $g^{(2)}$ is more robust, since the density is a less sensitive measure of the system. To substantiate our systematic procedure, further details on the sensitivity of the density fluctuation results to the energy cutoff are given in Appendix A, where it is demonstrated that a variation of 30% either side of our result leads to results that fall outside of the experimental error bars. Moreover, Appendix B gives a modified form of Eq. (1) which allows results for a given energy cutoff to be obtained irrespective of the spatial discretization choice made in the numerical simulations.

An important feature of Ref. [13] was the experimental demonstration of scale invariance in a 2D Bose gas. Plotting their data against a scaled chemical potential, $\beta(\mu - V(r))$, Hung *et al.* showed that densities measured at several temperatures collapsed to a single curve when appropriately scaled to the thermal de Broglie wavelength, λ_{dB}. This was found to be true in both the thermal and the superfluid regimes; the fluctuation region may be identified with the crossover from a thermal gas to a superfluid, where the system moves from an enhancement to a suppression of density fluctuations, respectively, as shown in the lower rightmost plot in Fig. 2. An important difference between the MP and the SGPE approaches, therefore, is the discontinuity in the density predicted by the former. In contrast, a key strength of the

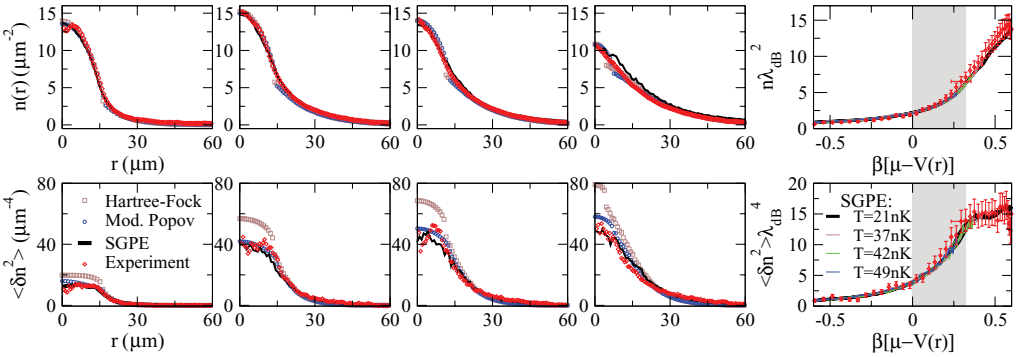

FIG. 2. (Color online) Density (top) and density fluctuations (bottom) from the SGPE, modified Popov (Bose-Einstein), and Hartree-Fock calculations versus the experimental data from Ref. [13]. The rightmost plots show that the SGPE results capture the experimentally observed scale invariance found in Ref. [13], including across the transition region indicated by the shaded (gray) area.

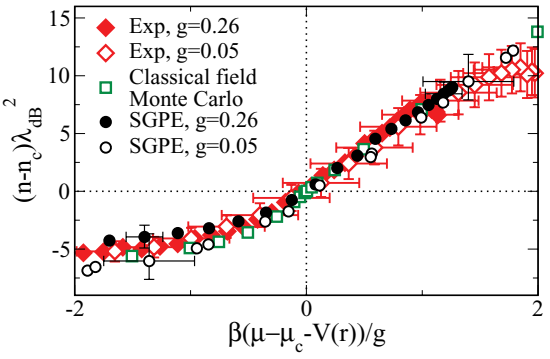

FIG. 3. (Color online) Universal behavior of shifted density profiles $(n - n_c)\lambda_{dB}^2$ versus rescaled chemical potential $\beta(\mu - \mu_c - V(r))/g$. Indicative error bars are shown for several SGPE data points which originate from the fit used to obtain μ_c.

SGPE lies in its applicability across this fluctuation region, as shown in the rightmost plots in Fig. 2, which show that it also demonstrates scale invariance in good agreement with the experimental data.

To estimate the location of the BKT transition from the SGPE simulations, we employ the fitting function used by Hung *et al.*, which yields a critical chemical potential, μ_c, and a corresponding critical density, n_c. These parameters can then be used to uncover the universal physics of 2D Bose gases, since close to the transition point, the shifted density $(n - n_c)\lambda_{dB}^2$ should be a universal function of $(\mu - \mu_c)\beta/g$ alone [13,14]. The universality of 2D Bose gases may then be tested by comparing scaled densities from gases with different interaction strengths, as in Ref. [13]. As shown in Fig. 3, by doing so we find that the SGPE reproduces the expected universal behavior demonstrated experimentally. Moreover, we compare it to the classical field MC results in Ref. [14], again finding good agreement.

Finally, to examine more closely how well the experimentally observed correlation effects are captured by the SGPE, we compare the density fluctuations to the compressibility. The compressibility may be calculated from the experimental data and SGPE using the expression $\kappa = \partial\langle n\rangle/\partial\mu_{eff}$, the results of which are shown in Fig. 4; once again, they closely follow the results in Ref. [13].

IV. CONCLUSIONS

We have found excellent agreement between *ab initio* calculations based on the stochastic Gross-Pitaevskii and MP theories with *in situ* experimental data from the 2D Bose gas experiments of Hung *et al*. Combining these two methods, we have devised and tested a systematic approach to the problem of cutoff choice within classical field simulations that could prove crucial in modeling out-of-equilibrium scenarios, which offer a natural extension to the present work.

ACKNOWLEDGMENTS

We thank Chen-Lung Hung and the other members of the Cheng Chin group for supplying us with their data and for useful discussions. We acknowledge funding from the EPSRC through Grant No. EP/F055935/1.

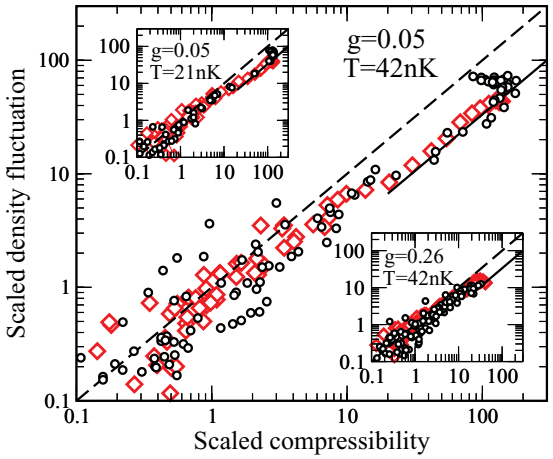

FIG. 4. (Color online) Scaled density fluctuation, $\langle\delta\tilde{n}^2\rangle = \lambda_{dB}^4\langle\delta n^2\rangle$, versus the scaled compressibility, $\tilde{\kappa} = \lambda^2\kappa/\beta$ from SGPE (black circles) and experiment (red diamonds). Dashed and solid lines show $\langle\delta\tilde{n}^2\rangle = \tilde{\kappa}$ and $\langle\delta\tilde{n}^2\rangle = \tilde{\kappa}/3$ respectively.

APPENDIX A: SENSITIVITY OF DENSITY FLUCTUATIONS TO THE ENERGY CUTOFF

This Appendix provides further evidence of the suitability of our method for finding an "optimum" cutoff, by investigating the sensitivity to cutoff choice of theoretical predictions for experimentally measurable properties. We focus here on the scale-invariant density fluctuation plot in Fig. 2 (bottom row, rightmost image) and calculate the density fluctuations that arise for several cutoffs around the value obtained using the combined SGPE-MP approach to cutoff choice. The results of this are reported in Fig. 5 and show that, while the difference between cutoffs is not as apparent in the thermal region, the data in the quasicondensate region $[\beta(\mu - V(r)) \gtrsim 0.25]$ indicate that a variation of about 30% in either direction in the energy cutoff is sufficient to give results that fall outside of the experimental error bars. For comparison, a 30% variation in the energy cutoff corresponds to the range

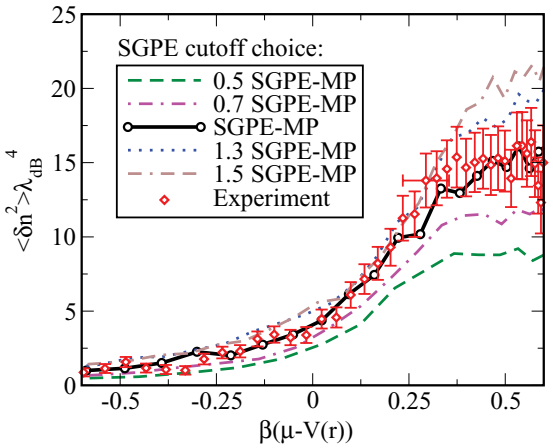

FIG. 5. (Color online) Scaled density fluctuations obtained from the SGPE for several energy cutoffs around the SGPE-MP result. Experimental error bars correspond to a variation of about 30% around the SGPE-MP energy cutoff, illustrating the range of cutoffs that would be consistent with the experimental data.

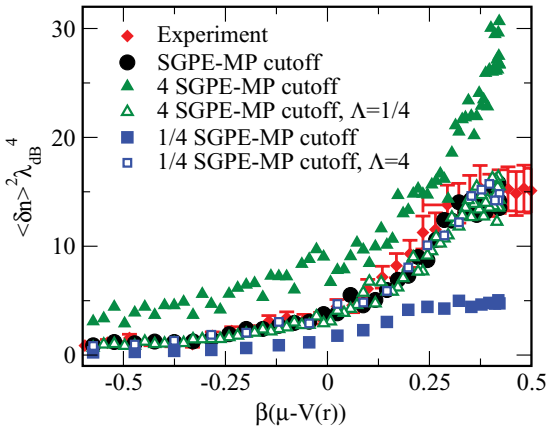

FIG. 6. (Color online) Scaled density fluctuations obtained for several energy cutoffs, where the cutoff is determined either directly by the grid spacing (filled symbols) or with $\Lambda \neq 1$ in Eq. (B1) (open symbols). The effect of the parameter Λ in mapping the results for one grid spacing to the results of another is shown, illustrating that the dependence of the energy cutoff upon the grid spacing may be removed for equilibrium calculations.

$0.54k_BT \leqslant E_{\rm cut} \leqslant k_BT$. The cutoff value found to give the best agreement for the ideal-gas case, $\beta E_{\rm cut} \approx 1.6$ [48], would correspond to an increase of about 108% relative to the value found using the SGPE-MP method and, therefore, would lie outside of the experimental error range.

APPENDIX B: REMOVING THE DEPENDENCE OF THE ENERGY CUTOFF UPON THE NUMERICAL GRID SPACING IN THE SGPE

This Appendix discusses a means for extracting grid-independent results for a chosen cutoff using the SGPE. Solving the SGPE in the form of Eq. (1) using an approach based upon a finite difference scheme, such as that described for a one-dimensional gas in Ref. [32], leads to a direct dependence of the ultraviolet energy cutoff upon the numerical grid spacing used [i.e., $E_{\rm cut} \propto 1/(\Delta x)^2$]. This direct dependence was used to specify the cutoff used in obtaining the results presented elsewhere in this paper. Interestingly, however, we note here that this link between grid spacing and energy cutoff may be removed for equilibrium calculations, by solving a heuristically modified form of the SGPE:

$$i\hbar\frac{\partial\psi(\mathbf{x},t)}{\partial t} = [1 - i\gamma(\mathbf{x},t)]\Big[-\frac{\Lambda\hbar^2}{2m}\nabla^2_{\rm x,y} + V(\mathbf{x}) - \mu + g_{\rm 2D}(|\psi(\mathbf{x},t)|^2 + 2n_{\rm above}(\mathbf{x}))\Big]\psi(\mathbf{x},t) + \sqrt{\Lambda}\eta(\mathbf{x},t). \quad \text{(B1)}$$

Here, Λ is a parameter that may be used to map the results for one grid spacing to those of another, i.e., setting $\Lambda \neq 1$ leads to a result which corresponds to a different energy cutoff, relative to that which would otherwise be expected for a given grid. The effect of this parameter is to offset the change in the kinetic energy term of the SGPE that would be caused when altering the numerical grid spacing. This parameter then also offers a means of control over the effective cutoff in simulations that does not rely upon altering the grid spacing.

For example, halving the grid spacing would ordinarily increase the energy cutoff by a factor of 4, however, this may be canceled out by setting $\Lambda = 1/4$. An example of this effect is shown in Fig. 6, where the results obtained using the grid corresponding to the SGPE-MP "optimum" cutoff are compared with those obtained using two other grid spacings, which are half and double this size, respectively. Clearly the unaltered results (i.e., setting $\Lambda = 1$ for all grids) are very different, particularly in the case of the density fluctuations. However, selecting an appropriate value for Λ, in order to cancel the effect of changing the grid spacing upon the energy cutoff, leads to a single consistent curve for all grids.

More generally, if the grid is changed such that $\Delta x, \Delta y \rightarrow \alpha\Delta x, \alpha\Delta y$, then setting $\Lambda = \alpha^2$ leads to the same equiliubrium result as would be obtained for the original grid with $\Delta x, \Delta y$. This method is somewhat analogous to the established technique of adding counter terms to remove divergences in lattice field theories; see, for example, Refs. [51,52]. Note, finally, that the cutoff used elsewhere in this paper was specified via the grid spacing directly, so results presented outside of this Appendix were not obtained by making use of Eq. (B1) with $\Lambda \neq 1$.

[1] I. Bloch, J. Dalibard, and W. Zwerger, Rev. Mod. Phys. **80**, 885 (2008).
[2] N. D. Mermin and H. Wagner, Phys. Rev. Lett. **17**, 1133 (1966).
[3] P. C. Hohenberg, Phys. Rev. **158**, 383 (1967).
[4] Z. Hadzibabic, P. Krüger, M. Cheneau, B. Battelier, and J. Dalibard, Nature (London) **441**, 1118 (2006).
[5] V. Schweikhard, S. Tung, and E. A. Cornell, Phys. Rev. Lett. **99**, 030401 (2007).
[6] P. Krüger, Z. Hadzibabic, and J. Dalibard, Phys. Rev. Lett. **99**, 040402 (2007).
[7] Z. Hadzibabic, P. Krüger, M. Cheneau, S. P. Rath, and J. Dalibard, New J. Phys. **10**, 045006 (2008).
[8] P. Cladé, C. Ryu, A. Ramanathan, K. Helmerson, and W. D. Phillips, Phys. Rev. Lett. **102**, 170401 (2009).
[9] S. Tung, G. Lamporesi, D. Lobser, L. Xia, and E. A. Cornell, Phys. Rev. Lett. **105**, 230408 (2010).
[10] S. P. Rath, T. Yefsah, K. J. Günter, M. Cheneau, R. Desbuquois, M. Holzmann, W. Krauth, and J. Dalibard, Phys. Rev. A **82**, 013609 (2010).
[11] T. Yefsah, R. Desbuquois, L. Chomaz, K. J. Günter, and J. Dalibard, Phys. Rev. Lett. **107**, 130401 (2011).
[12] T. Plisson, B. Allard, M. Holzmann, G. Salomon, A. Aspect, P. Bouyer, and T. Bourdel, Phys. Rev. A **84**, 061606 (2011).
[13] C.-L. Hung, X. Zhang, N. Gemelke, and C. Chin, Nature **470**, 236 (2011).
[14] N. Prokof'ev and B. Svistunov, Phys. Rev. A **66**, 043608 (2002).
[15] A. Posazhennikova, Rev. Mod. Phys. **78**, 1111 (2006).
[16] V. L. Berezinskii, Sov. Phys. JETP **34**, 610 (1972).

[17] J. M. Kosterlitz and D. J. Thouless, J. Phys. C **6**, 1181 (1973).
[18] Y. Kagan, V. A. Kashurnikov, A. V. Krasavin, N. V. Prokof'ev, and B. V. Svistunov, Phys. Rev. A **61**, 043608 (2000).
[19] N. Prokof'ev, O. Ruebenacker, and B. Svistunov, Phys. Rev. Lett. **87**, 270402 (2001).
[20] M. Holzmann and W. Krauth, Phys. Rev. Lett. **100**, 190402 (2008).
[21] C. Gies, B. P. van Zyl, S. A. Morgan, and D. A. W. Hutchinson, Phys. Rev. A **69**, 023616 (2004).
[22] C. Gies and D. A. W. Hutchinson, Phys. Rev. A **70**, 043606 (2004).
[23] L.-K. Lim, C. M. Smith, and H. T. C. Stoof, Phys. Rev. A **78**, 013634 (2008).
[24] M. Holzmann, M. Chevallier, and W. Krauth, Europhys. Lett. **82**, 30001 (2008).
[25] R. N. Bisset and P. B. Blakie, Phys. Rev. A **80**, 045603 (2009).
[26] T. P. Simula, M. J. Davis, and P. B. Blakie, Phys. Rev. A **77**, 023618 (2008).
[27] R. N. Bisset, M. J. Davis, T. P. Simula, and P. B. Blakie, Phys. Rev. A **79**, 033626 (2009).
[28] R. N. Bisset and P. B. Blakie, Phys. Rev. A **80**, 035602 (2009).
[29] J. O. Andersen, U. Al Khawaja, and H. T. C. Stoof, Phys. Rev. Lett. **88**, 070407 (2002).
[30] U. Al Khawaja, J. O. Andersen, N. P. Proukakis, and H. T. C. Stoof, Phys. Rev. A **66**, 013615 (2002); **66**, 059902(E) (2002).
[31] H. T. C. Stoof, J. Low Temp. Phys. **114**, 11 (1999).
[32] H. T. C. Stoof and M. J. Bijlsma, J. Low Temp. Phys. **124**, 431 (2001).
[33] R. A. Duine and H. T. C. Stoof, Phys. Rev. A **65**, 013603 (2001).
[34] C. W. Gardiner and M. J. Davis, J. Phys. B **36**, 4731 (2003).
[35] S. P. Cockburn, D. Gallucci, and N. P. Proukakis, Phys. Rev. A **84**, 023613 (2011).
[36] D. Gallucci, S. P. Cockburn, and N. P. Proukakis, Phys. Rev. A **86**, 013627 (2012).
[37] S. P. Cockburn, H. E. Nistazakis, T. P. Horikis, P. G. Kevrekidis, N. P. Proukakis, and D. J. Frantzeskakis, Phys. Rev. Lett. **104**, 174101 (2010).
[38] S. P. Cockburn and N. P. Proukakis, Las. Phys. **19**, 558 (2009).
[39] P. B. Blakie, A. S. Bradley, M. J. Davis, R. J. Ballagh, and C. W. Gardiner, Adv. Phys. **57**, 363 (2008).
[40] P. Arnold and G. Moore, Phys. Rev. Lett. **87**, 120401 (2001).
[41] L. Zawitkowski, M. Brewczyk, M. Gajda, and K. Rzażewski, Phys. Rev. A **70**, 033614 (2004).
[42] L. Giorgetti, I. Carusotto, and Y. Castin, Phys. Rev. A **76**, 013613 (2007).
[43] The density of atoms with momenta higher than the grid cutoff, n_{above}, is calculated iteratively, in the Hartee-Fock limit, prior to carrying out the SGPE simulations using the density from the MP theory based upon Rayleigh-Jeans statistics.
[44] N. P. Proukakis, Phys. Rev. A **74**, 053617 (2006).
[45] S. P. Cockburn, A. Negretti, N. P. Proukakis, and C. Henkel, Phys. Rev. A **83**, 043619 (2011).
[46] V. N. Popov, *Functional Integrals in Quantum Field Theory and Statistical Physics* (Reidel, Dordrecht, 1983).
[47] As in the SGPE, we also include the atoms with momenta above the cutoff in the classical case of the MP. For the "optimum" cutoff, we find this number of atoms to be a small fraction of the total, which we retain mainly for completeness.
[48] E. Witkowska, M. Gajda, and K. Rzażewski, Phys. Rev. A **79**, 033631 (2009).
[49] While the chemical potential is fixed between the SGPE and the modified Popov calculations, we find a different value of μ must be used in order to match the Hartree-Fock density to the experimental central density. The temperature, however, remains fixed in all methods.
[50] J.-B. Trebbia, J. Esteve, C. I. Westbrook, and I. Bouchoule, Phys. Rev. Lett. **97**, 250403 (2006).
[51] M. Gleiser and H.-R. Müller, Phys. Lett. B **422**, 69 (1998).
[52] L. M. A. Bettencourt, S. Habib, and G. Lythe, Phys. Rev. D **60**, 105039 (1999).